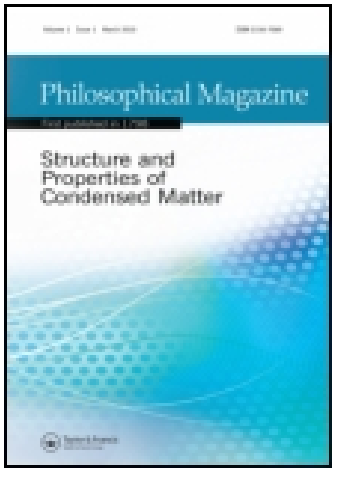

Philosophical Magazine
Publication details, including instructions for authors and subscription information:
http://www.tandfonline.com/loi/tphm20

Mild degradation processes in ZnO-based varistors: the role of Zn vacancies

M.A. Ponce[a], C. Macchi[bc], F. Schipani[a], C.M. Aldao[a] & A. Somoza[bd]

[a] Institute of Materials Science and Technology (INTEMA), University of Mar del Plata and National Research Council (CONICET), Juan B. Justo 4302, B7608FDQ Mar del Plata, Argentina

[b] Instituto de Física de Materiales Tandil (IFIMAT), CIFICEN, Consejo Nacional de Investigaciones Científicas y Técnicas (CONICET) y Universidad Nacional del Centro de la Provincia de Buenos Aires, Pinto 399, B7000GHG Tandil, Argentina

[c] CONICET, Buenos Aires, Argentina

[d] Consejo de Investigaciones Científicas de la Provincia de Buenos Aires, La Plata, Argentina

Published online: 09 Feb 2015.

To cite this article: M.A. Ponce, C. Macchi, F. Schipani, C.M. Aldao & A. Somoza (2015) Mild degradation processes in ZnO-based varistors: the role of Zn vacancies, Philosophical Magazine, 95:7, 730-743, DOI: 10.1080/14786435.2015.1006291

To link to this article: http://dx.doi.org/10.1080/14786435.2015.1006291

Philosophical Magazine, 2015
Vol. 95, No. 7, 730–743, http://dx.doi.org/10.1080/14786435.2015.1006291

Mild degradation processes in ZnO-based varistors: the role of Zn vacancies

M.A. Ponce[a]*, C. Macchi[b,c], F. Schipani[a], C.M. Aldao[a] and A. Somoza[b,d]

[a]*Institute of Materials Science and Technology (INTEMA), University of Mar del Plata and National Research Council (CONICET), Juan B. Justo 4302, B7608FDQ Mar del Plata, Argentina;* [b]*Instituto de Física de Materiales Tandil (IFIMAT), CIFICEN, Consejo Nacional de Investigaciones Científicas y Técnicas (CONICET) y Universidad Nacional del Centro de la Provincia de Buenos Aires, Pinto 399, B7000GHG Tandil, Argentina;* [c]*CONICET, Buenos Aires, Argentina;* [d]*Consejo de Investigaciones Científicas de la Provincia de Buenos Aires, La Plata, Argentina*

(*Received 20 July 2014; accepted 18 December 2014*)

The effects of a degradation process on the structural and electrical properties of ZnO-based varistors induced by the application of *dc* bias voltage were analysed. Capacitance and resistance measurements were carried out to electrically characterize the polycrystalline semiconductor before and after different degrees of mild degradation. Vacancies' changes in the varistors were studied with positron annihilation lifetime spectroscopy. Variations on the potential barrier height and effective doping concentration were determined by fitting the experimental data from impedance spectroscopy measurements. These results indicate two different stages in the degradation process consistent with vacancy-like concentration changes.

Keywords: zinc oxide; varistors; degradation; impedance spectroscopy; positron annihilation lifetime spectroscopy

Introduction

The bulk resistivity of ZnO cannot account for the observed electrical conductivity of polycrystalline materials. In fact, electrical properties of polycrystalline semiconductors are known to be dominated by potential barriers at the grain boundaries [1,2]. Thus, the high resistivity exhibited at low applied voltages derives from grain boundaries since grains are very conductive. At high enough applied voltage, a breakdown of these intergranular barriers takes place and the conductivity rapidly increases in a narrow range of the applied voltage. This characteristic constitutes the working principle of metal-oxide varistors, used as circuit protection [3–8]. Potential barriers are caused by intergrain states that may arise due to the presence of impurity or additive atoms, or to dislocations introduced by the crystallographic mismatch between adjacent grains, or because of an intergranular layer, which is another oxide. Regardless of their origin, interface states deplete carriers from surrounding grains leading to the formation of double Schottky barriers.

*Corresponding author. Email: mponce@fi.mdp.edu.ar

ZnO varistors are known to exhibit degradation in electrical characteristics when stressed by an electric field [9–12]. Indeed, they exhibit an increase in leakage current when subjected to a constant applied voltage. This degradation has been widely studied, and several mechanisms, including electron trapping, dipole orientation, ion-migration and oxygen desorption, have been proposed to explain this phenomenon. Among these, the ion-migration model has found the most experimental support. This mechanism assumes the presence of positively charged zinc interstitials in the depletion layer and negatively charged zinc vacancies at the grain boundary. The degradation phenomenon is associated with the drift of positively charged zinc interstitial ions from the interior of the grain to the grain boundary. At odds with this model, we have systematically found that, after degradation, the donor concentration increases implying an increase in the oxygen vacancy concentration.

In this study, we estimated variations on barrier height and doping concentration from impedance spectroscopy measurements and positron annihilation spectroscopy (PAS) in ZnO-degraded commercial varistors. We found that a mild degradation, after electric field stress, leads to a reduction in barrier heights and of the effective doping concentration at the grains, as stated regularly in the ion-migration model. Conversely, a stronger degradation leads to an increase of the effective doping that we have reported in the past [13].

Positron annihilation spectroscopy

PAS is a powerful non-destructive tool for studying open-volume defects in solids [14–16], it can provide invaluable information regarding processes associated with degradation. Among the different experimental variants of PAS, positron annihilation lifetime spectroscopy (PALS) has demonstrated to be the most suitable technique to get information about type and concentration of vacancy-like defects [16]. Taking into account the nature of the studied material in this study, a comprehensive review on the use of positrons to study semiconductors can be found in Ref. [17]. In particular, when a positron enters in a semiconductor material, it loses its kinetic energy rapidly and reaches thermal equilibrium with the crystal lattice. After thermalization, the positron annihilates directly from the delocalized state with an electron or can be trapped by a vacancy-like defect and then the e^+–e^- pair annihilates at a localized state. It is well known that positron lifetime correlates with the open volume associated with the annihilation trap; thus, it is longer at vacancy defects than in the delocalized state in the lattice. Neutral and negatively charged vacancies are efficient positron traps due to the missing positive ion core. In the literature, there are only few studies on commercial ZnO-based varistors using PAS. For example, Gupta et al. characterized the defect state of a ZnO commercial varistor submitted to different thermal treatments [18]. The obtained results allowed the authors to validate their grain-boundary defect model mentioned in the introduction. In a previous study, this research group investigated the same type of varistors to study the influence of the time and applied bias on the concentration of vacancy-like defects at the grain boundaries [19]. In this pioneering work, PALS and electrical current measurements were jointly used to study the grain-boundary defect changes during electrically induced degradation of the varistors.

On the other hand, detailed information dealing with native defects in ZnO pure crystals was reported (see for example Refs. [20–32]). Specifically, PAS techniques

allowed Tuomisto and co-workers to report that in as-grown undoped ZnO crystals grown by the seeded vapour phase technique (SVPT), the dominant acceptors are the Zn vacancies (V_{Zn}) [22,23]. Furthermore, these authors found three different types of vacancy-like defects were produced in *n*-type ZnO single crystals after electron irradiation: V_{Zn} and O vacancies (V_O) (or complexes involving these vacancies) and negative-ion-type defects, which are attributed to O interstitials or O antisites. The V_{Zn} and negative-ion-type defects acted as compensating centres. In the case of V_O, they were revealed as a neutral vacancy-like defect with a deep donor character.

Conduction through a double Schottky potential barrier

Usually, the electrical properties of polycrystalline semiconductors are described with a double one-dimensional barrier representing the interface between two grains [33]. The semiconductor is assumed to be homogeneous up to the grain boundary, so that the uncompensated donors give rise to a uniform space charge in the depletion region. The electric field therefore increases linearly with distance from the edge of the depletion region, and the electrostatic potential is quadratic resulting in a parabolic barrier known as the Schottky barrier. The scheme of Figure 1 shows an *n*-type semiconductor junction before and after the degradation process. Oxygen vacancies at the depletion regions behave as donors, while zinc vacancies behave as acceptors [34,35]. (Changes due to degradation will be discussed below.)

Regularly, it is considered that the carrier transport through grain boundaries is thermionic. If so, the electron current density from the negatively biased grain to the positively biased grain would be [36–38]

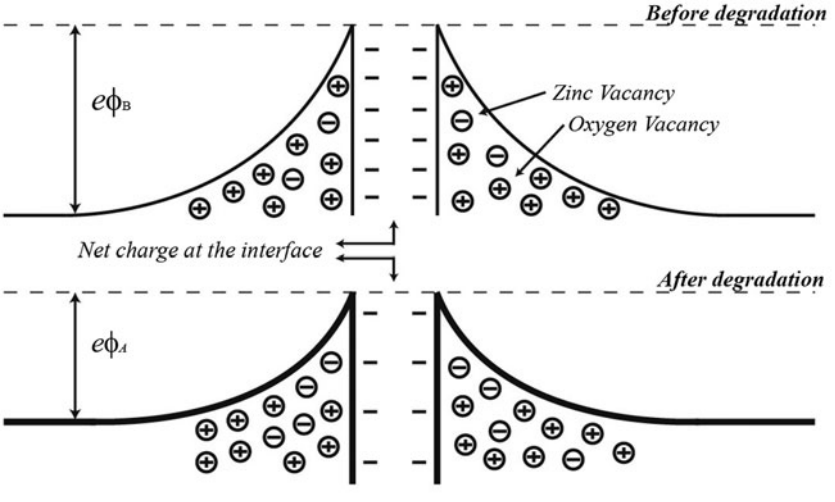

Figure 1. The diagram shows schematically the degradation process in the intergrain and the depletion zones that constitute the double Schottky barrier model. As a result of Zn migration to the grain boundaries, charge at the interface is lower reducing the barrier height and the effective doping concentrations at the depletion regions decreases after degradation.

$$J_{\text{th}} = AT^2 \exp[-(e\phi + \xi)/kT] \quad (1)$$

where A is the Richardson constant, T the temperature, k the Boltzmann constant and ξ the difference between the conduction band minimum and the Fermi level at the bulk. Strictly, the Schottky barrier height, $e\phi$, should be defined as the difference between the top of the barrier and the Fermi level. However, many researchers in the field define the barrier height as the band bending, i.e. the difference between the top of the barrier and the bottom of the conduction band in the bulk. We adopted this convention here. For low doping concentrations and high temperatures, the tunnelling current contribution is not significant, and does not change the analysis (for a detail, study of this type of conduction mechanism see Ref. [38]).

Materials and methods

Experimental measurements carried out on commercial varistors GNR14D470 K (14 mm diameter) are reported. An X-ray diffraction (XRD) analysis was performed with a Philips (PW1830) diffraction system employing CuKα radiation at 40 kV and 40 mA. Samples were scanned between 20° and 80° with a step size of 0.01°. XRD data were analysed using the X'Pert PRO HighScore software, and the crystallographic files correspond to codes 01-079-2205, 00-027-0053 and 01-075-00343 of the International Center for Diffraction Data Powder diffraction file database [Newtown Square, USA (1998)]. As shown in the diffractogram, the main component corresponds to ZnO, code 01-079-2205, traces of Bi_2O_3, code 00-027-0053 and $Fe_2Mn_3O_8$, code 01-075-00343. Results before and after mild degradation show no detectable differences (Figure 2).

Varistor thickness was measured with an optical microscope (≈1.14 mm) and, to image the varistors intergranular surfaces, a JEOL JSM 6460-S scanning electron microscope (SEM) was employed. The average thickness is shown in Figure 3 in which a micrograph of the cross section is presented. The average grain size was determined to be ≈35 μm, using SEM as shown in Figure 4.

Thus, the average number of grains between contacts was $n \approx 32$. The same varistors were used for every set of measurements in order to decrease experimental errors, as a consequence of the possible composition variation in the commercial varistors.

The degradation occurs due to continuous leakage current that crosses the polycrystalline samples during the test. We applied two different types of electrical stress to mildly degrade the varistors: 50 mA (lower current intensity, LCI) for 6 h and 120 mA for 6 h (higher current intensity, HCI). The electrical stress was applied with both polarities. Capacitance measurements were carried out with a Hewlett Packard impedance analyzer model 4184A. A furnace, with a commercial temperature controller Novocontrol BDS 1200, was used for heating the samples.

PALS measurements were performed with a fast–fast spectrometer with a time resolution of 210 ps in a collinear geometry. As positron source, a 10 μCi sealed source of ^{22}NaCl deposited onto two thin Kapton foils (7.5 μm thick) sandwiched between two identical varistors samples was used. PALS spectra were acquired at *RT*, and typically, ~1.5–2 × 10^6 counts per spectra were collected. The lifetime reported in this work for each sample is at least an average of ten measurements in the same experimental condition. After subtracting the background and the source contribution, the lifetime spectra

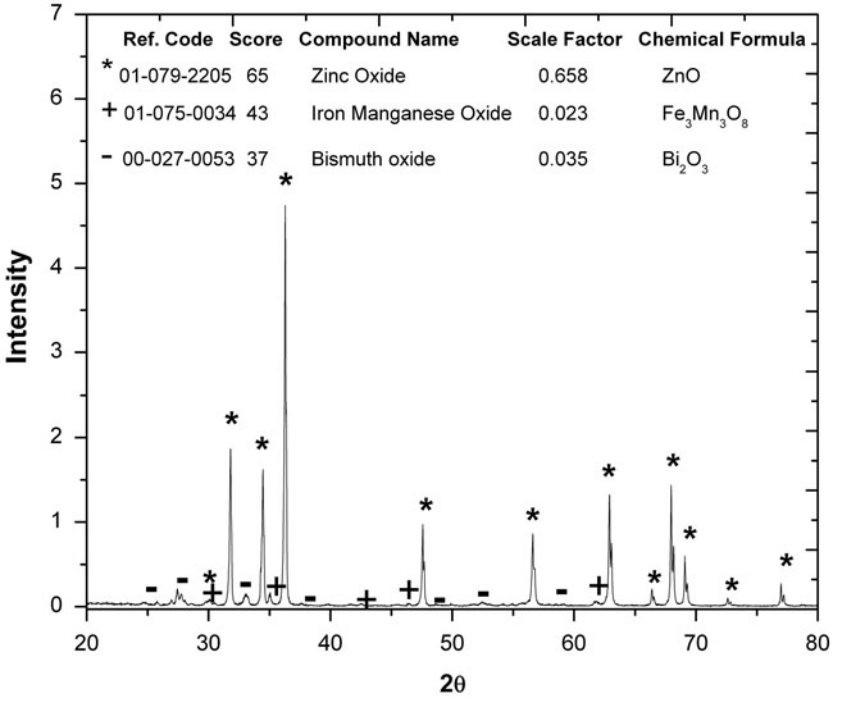

Figure 2. XRD spectrum corresponding to un-degraded sample. Results indicate that ZnO is the main compound with small amounts of Bi_2O_3 and $Fe_2Mn_3O_8$.

were analysed as the sum of an exponential decay convoluted with the Gaussian resolution function of the spectrometer, i.e. $n(t) = \sum_i I_i \exp(-t/\tau_i)$, where the positron in the state i annihilates with a characteristic lifetime τ_i and an associated intensity I_i. The state i can be the delocalized state in the crystal lattice (bulk state) or a localized state at a defect site. It is well known that the most statistically robust parameter is the positron mean lifetime ($\bar{\tau}$) defined as the sum of the individual lifetimes weighted with the normalized intensity of each lifetime component, $\bar{\tau} = \sum_i I_i \tau_i$. The increase of $\bar{\tau}$ above the bulk positron lifetime (τ_b) indicates that defects are present in the sample. Lifetime spectra were analysed using the POSITRONFIT program [39]. In all cases, and as usual when studying semiconductors [17], PALS spectra were satisfactorily fitted using two lifetime components. In this scenario, positron can be trapped and then annihilated in only one type of defect which is characterized with the second lifetime component τ_2 and its associate intensity I_2, and the short-lived positron lifetime τ_1 represents the reduced positron lifetime in the bulk state (see Equation (3)).

To obtain the defect concentration, PALS results were analysed into the frame of the one-defect simple trapping model (STM) [14,17,40]. The simplified STM was proposed as an approximation 'adequate in most cases' of positron trapping under the transition-limited regime [40,41]. As discussed in detail in Ref. [41] and references therein, STM can be well used when positrons are annihilated in polycrystalline materials with typical grain sizes higher than about 10 μm. For lower grain sizes, STM is a bad

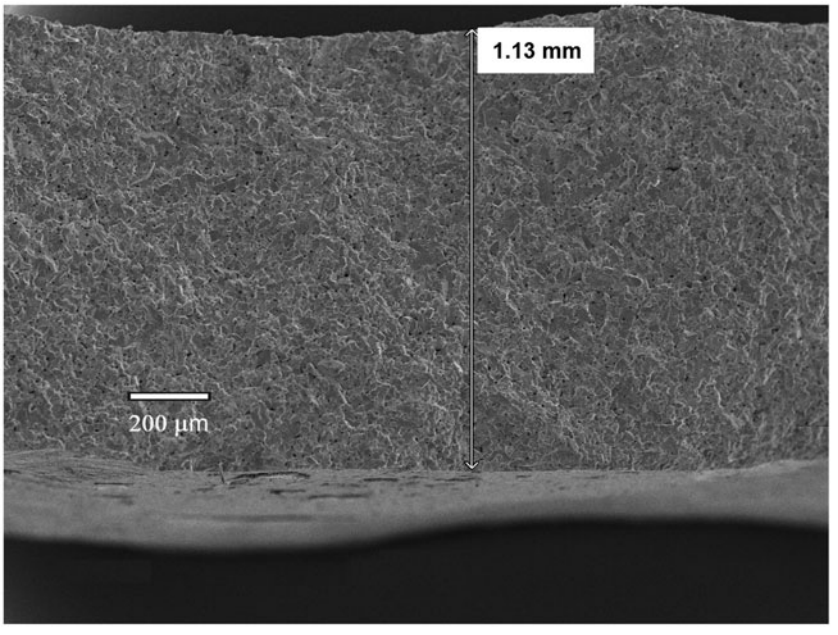

Figure 3. SEM image of the un-degraded varistor cross-section. The thickness measured was 1.13 mm.

approximation since positron trapping at grain boundaries is limited by transport. In such a case, the diffusion-trapping model must be used (see Refs [41,42]).

The characteristic parameters of the STM are as follows: (1) the bulk positron lifetime τ_b, (2) the positron lifetime in the defect τ_d, and (3) the rate at which positrons are trapped by the defect state (positron trapping rate, κ_d). κ_d is proportional to the defect concentration C_d, i.e. $\kappa_d = (\mu_d/N_{at})C_d$ where the specific positron trapping coefficient μ_d depends on the type of defect and its charge state [14,17], and N_{at} is the atomic density of the material. The solution of the differential equations resulting from the STM gives the following relationships between the experimental values τ_i and I_i and the characteristic parameters τ_b, τ_d and κ_d:

$$\tau_d = \tau_2 \tag{2}$$

$$\tau_b^{-1} = I_1\tau_1^{-1} + i_2\tau_2^{-1} \tag{3}$$

$$k_d = \frac{\mu_d}{N_{at}}C_d = \tau_b^{-1}\left(\frac{\bar{\tau} - \tau_b}{\tau_d - \bar{\tau}}\right) \tag{4}$$

The validity of the model used above can be tested calculating τ_b from the decomposition of the experimental spectra using Equation (3) and compare it to τ_b measured experimentally. If there is a significant difference (>5 ps), more than one type of positron traps exist in the sample (see details in Ref. [14]).

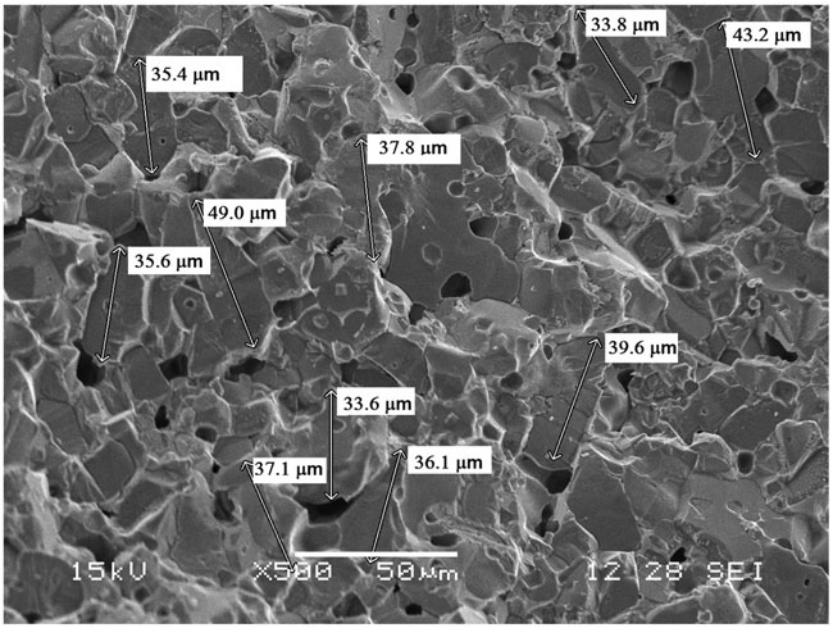

Figure 4. SEM image of the un-degraded sample. In the image, different bars indicating the typical dimension of the grain sizes were drawn.

Results and discussion

Vacancy-like defect concentration before and after degradation

The analysis of the PALS spectra for all the samples studied consisted on two steps. In the first, a free constraint fitting analysis revealed the presence of an almost constant second positron lifetime τ_2. Then, as usual, a subsequent analysis was carried out by fixing τ_2 at the value resulting from averaging ten lifetimes. A summary of the main results obtained is shown in Table 1.

For the un-degraded and in the LCI degraded samples, $\tau_2 = 240 \pm 5$ ps. In recent studies on electron irradiated undoped ZnO crystals grown by SVPT [22,23], electron irradiated ZnO hydrothermal growth single crystals [24] and ZnO crystals grown by the contactless chemical vapor transport (CVT) method [27], a value for the second lifetime component of 230 ± 10 ps was reported. In all cases, this lifetime was associated with

Table 1. Characteristic positron lifetimes and their associated intensities (I_1 (%) = 100 − I_2) obtained from the decomposition of PALS spectra. $\bar{\tau}$ represents the positron mean lifetime (see text). *F* indicates that the corresponding lifetime value was fixed for a further analysis of PALS spectra.

Samples		τ_1 (ps)	τ_2 (ps)	I_2 (%)	$\bar{\tau}$ (ps)
Before degradation		167 ± 1	240 F	21.0 ± 0.5	182.5 ± 0.5
After degradation	LCI	157 ± 1	240 F	32.6 ± 0.5	184.5 ± 0.5
	HCI	162 ± 1	270 F	20.9 ± 0.5	184.7 ± 0.5

positrons annihilated in negatively charged Zn monovacancies (V_{Zn}). On the other hand, the same lifetime value was reported when measuring as-grown undoped and Mn-doped ZnO crystals grown by the CVT method; in this case, the positron traps were identified as neutral Zn-vacancy-related complexes [28]. Within the experimental scatter, the reported τ_2 in the mentioned studies show a very good agreement with our results obtained for the un-degraded and LCI varistors. It must also be taken into account that ZnO samples usually contain oxygen vacancies (V_O) [18,19]; however, it has been reported that at room temperature, positrons are not sensitive to the presence of this kind of defects [22]. Under this scenario, it can be concluded that in the un-degraded and LCI samples, positrons annihilate in V_{Zn}-like defects. From XRD measurements, we know that the studied commercial ZnO-based varistors contain traces of two kinds of metal oxides. Because of the very small content of these oxides in the samples, positron annihilation in these phases can be considered negligible.

In the case of the HCI samples, from the decomposition of the PALS spectra, a second lifetime component of 270 ± 5 ps was obtained. This τ_2 value is about 10% higher than those we have obtained from the decomposition of the lifetime spectra measured in un-degraded and LIC samples. In general, it is well known that a longer lifetime, with respect to that of a monovacancy, means that positrons become trapped and annihilated in traps with greater sizes [14,17]. In the case of HCI degraded samples, the increase of ~10% in τ_2 would indicate that positrons are annihilating in defects with a typical size of a divacancy [43]. It must also be taken into account that similar τ_2 values were reported by several authors measuring: polycrystalline ZnO ceramic samples sintered at different temperatures [29], virgin ZnO single crystals grown using a pressurized melt growth approach [30,41] and proton irradiated ZnO single crystals grown by EaglePicher (EP) [32]. In all the cited works, the lifetime values varying between 255 and 265 ps were ascribed to positron annihilations in Zn + O divacancies (V_{Zn+O}). Recently, it has been reported that V_{Zn+O} is a deep positron trap and its calculated lifetime is 265 ps [44]. Consequently, in the case of HCI samples, the comparison between the τ_2 values (270 ± 5 ps) measured experimentally with those above specified experimental lifetime values and that obtained by *ab initio* calculations strongly indicates that positron traps are V_{Zn+O}.

As mentioned in Section 2, we experimentally tested the validity of the one-defect STM, the positron lifetime value for ZnO bulk was calculated using Equation (3) and the experimental values reported in Table 1. For all varistors studied, almost identical τ_b values were obtained (178 ± 2 ps). This value shows an excellent agreement with that we have obtained when measuring a well-annealed ZnO varistor (four cycles of 10 h at 800 °C followed by very slow cooling). Therefore, it can be concluded that the STM is a valid model to analyse the results reported in this study. Furthermore, it must be pointed out that our bulk lifetime for a commercial varistor shows a relative good agreement with those reported by Tuomisto ($\tau_b = 171$ ps) for ZnO crystals grown by SVPT [22] and EP [23], and Chen ($\tau_b = 183$ ps) for ZnO crystals hydrothermal growth single crystals [26]. On the other hand, Zhong et al. reported a $\tau_b = 183$ ps for sintered polycrystalline ZnO ceramic samples [29].

The concentrations of defects can be estimated from the trapping rates (Equation (4)), using the corresponding specific positron trapping coefficient μ_d and the atomic density of ZnO ($N_{at} = 8.3 \times 10^{28}\ 1/m^3$). As mentioned before, μ_d depends on the defect and on its charge state. Regarding the charge state, since our measurements were carried

out at room temperature, it is not possible to identify the defect charge state, i.e. whether they are neutral or negatively charged. In consequence, we assumed that all the revealed defects are in their neutral charge state.

For the un-degraded varistors, a V_{Zn}-like defect concentration C_{VZn} of ~2×10^{22} 1/m^3 was obtained, and for the LCI, C_{VZn} rises up to ~4×10^{22} 1/m^3. In both cases, the trapping coefficient for neutral vacancies in semiconductors $\mu_v^0 = 2 \times 10^{15} s^{-1}$[23] was used.

On the other hand, for the HCI samples, we have obtained the V_{Zn+O} divacancy concentration. In this case, a value for the trapping coefficient of divacancies twice of that corresponding to neutral vacancies in semiconductors [14], so $\mu_{2v}^0 = 4 \times 10^{15} s^{-1}$, was considered. As a result, a concentration of V_{Zn+O} divacancy of ~1×10^{22} 1/m^3 was derived.

Work in progress to measure the positron lifetime evolution in the low temperature region will allow us to determine the charge state of the defects present in the samples studied.

Potential barrier height and width dependence on degradation

The relationship between capacitance C and barrier height ϕ can be derived from Poisson's equation. According to the depletion approximation, the barrier height is given by [45]

$$\phi = \frac{eN_d w^2}{2\varepsilon} \tag{5}$$

and the capacitance per unit area by

$$C = \left(\frac{e\varepsilon N_d}{2\phi}\right)^{1/2} = \frac{\varepsilon}{w} \tag{6}$$

where e is the electron charge, ε the permittivity, N_d the donor concentration, $e\phi$ (given in eV) the barrier height and w is the width of the depletion region. Equation (6) shows that the capacitance corresponds to that of a parallel plate capacitor with a dielectric permittivity ε [45]. From Equation (6), we can obtain a relation between capacities before (B) and after (A) degradation:

$$\left(\frac{C_A}{C_B}\right)^2 = \frac{\phi_B N_A}{\phi_A N_B} \tag{7}$$

Figure 5 shows the capacitance before and after the LCI degradation process at 100 °C for a wide range of frequencies. A slight increase in the capacitance after the degradation process can be seen. The inset shows a fitting carried out with a capacitance in parallel with a constant phase element, which simulates the effect of traps. This was accomplished in the frequency range in which the grain boundary is dominant to avoid complexities such as electrode and bulk capacitances [46].

From the experiments presented in Figure 5, we found $(C_A/C_B)^2 = 1.095$, indicating an increase of dopant concentration, a decrease in the barrier height or a combined change after this mild degradation that leads to the observed capacitance increase.

As a first approach, we can consider that there is no variation of the donor concentration at the grain before and after degradation. From the resistivity changes presented in Figure 6, using Equation (1), the barrier height reduction after degradation could be

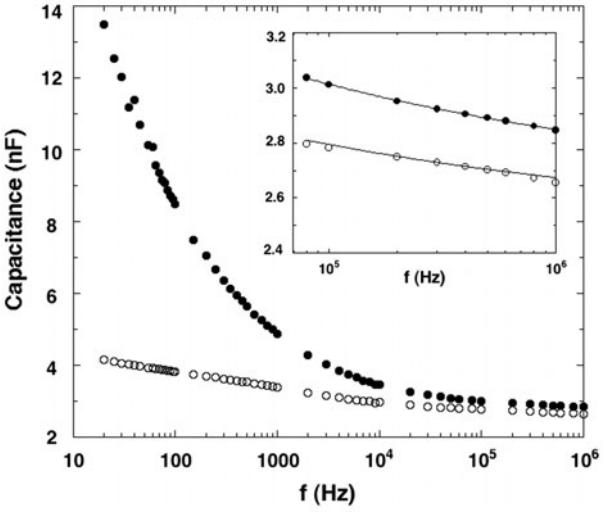

Figure 5. Capacitance as a function of frequency at $T = 373$ K. Empty symbols correspond to the varistor before degradation. Fittings were made in the higher frequency range with an equivalent circuit (a capacitance in parallel with a constant phase element, which simulates traps). The relation between the grain boundary capacitance after and before degradation $C_{\text{after/before}} \approx 1.05$, see Equation (7).

calculated, $\Delta\phi = 0.12$ V, and with the help of Equation (7) the barrier heights before and after degradation can be determined:

$$\begin{aligned} \phi_B &= 1.38 \text{ V} \\ \phi_A &= 1.26 \text{ V} \end{aligned} \tag{8}$$

In Figure 6, we present the conductivity as a function of the inverse temperature. Assuming that the main electronic transport mechanism is thermionic, Equation (1), barrier heights were obtained from the slopes resulting of the fit of the experimental data:

$$\begin{aligned} \phi_B &= 0.45 \text{ V} \\ \phi_A &= 0.29 \text{ V} \end{aligned} \tag{9}$$

Note that the barrier heights derived from conductance and capacitance, Equation (8), and conductance temperature dependence, Equation (9), are very different indicating an obvious inconsistency. This is a consequence of having assumed that the donor concentration before and after degradation remains unchanged. Results of Equations (8) and (9) show that the donor concentration is affected after degradation. Arrhenius plots for polycrystalline semiconductors are regularly sensitive to the temperature range used [47]. However, the discrepancy is so huge that the inconsistency cannot be avoided. For a more rigorous analysis, the tunnelling contribution to the electrical current could be considered [11–13,38,45]. However, in this case, due to the doping level and temperatures involved, results should not be significantly altered, and therefore the inconsistency could not be solved.

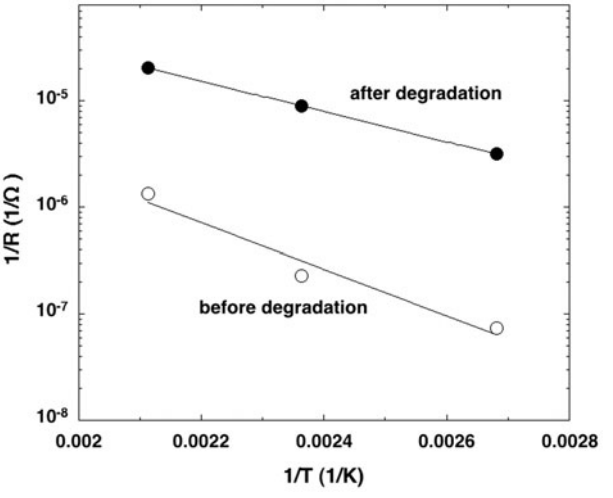

Figure 6. Arrhenius plot for the sample conductivities before and after degradation. Open symbols represent the values of conductivity at 373, 423 and 473 K before degradation and filled symbols after degradation. From the slopes and using Equation (1), barrier heights were determined: $e\phi_B = 0.43$ eV and $e\phi_A = 0.28$ eV. Solid lines correspond to the fittings considering a variation in the donor concentration and barrier heights. These were $e\phi_B = 0.47$ eV and $e\phi_A = 0.35$ eV and donor concentration $N_B = 5.7 \times 10^{23}$ 1/m^3 and $N_A = 4.6 \times 10^{23}$ 1/m^3. Error bars are within the size of the symbols.

New calculations were made from conductivity values based on the experimental capacities relation and considering a variation in barrier height $\Delta\phi = 0.12$ V, besides the donor concentration was set free. We could satisfactorily fit the experimental data with the following values for the barrier and the dopant concentration before and after LCI degradation by allowing a simultaneous change of barrier height and dopant concentration:

$$\begin{array}{ll} \phi_B = 0.47\text{V} & N_B = 5.7 \times 10^{23}\,1/\text{m}^3 \\ \phi_A = 0.35\text{V} & N_A = 4.6 \times 10^{23}\,1/\text{m}^3 \end{array} \tag{10}$$

Absolute values of the capacitance give confidence on the above results. The sample capacitance is that of a parallel plate capacitor. Assuming a homogeneous material, the capacitance would be $C = \varepsilon A/d = 6.67 \times 10^{-12}$ F, but the measured capacitance at 1 MHz is $C_{exp} = 2.8 \times 10^{-9}$ F. This difference can be attributed to an effective capacitance due to the presence of Schottky barriers. Indeed, the effective width is that due to depletion zones. So, the effective width relevant for the capacitance is $d_{eff} = 2wn$. Using Equations (5) and (6), we could estimate that the expected values for the donor concentration were about 5×10^{23} 1/m^3, which is consistent with the values determined from conductivity measurements.

For the LCI degraded samples, PALS results indicate a change in the vacancy-like defect concentration. In particular, it was observed that the density of V_{Zn} increases from ~2×10^{22} to ~4×10^{22} 1/m^3. At first sight, this variation is small but corresponds to an average measurement when it is known that the vacancy creation takes place mostly in a thin zone close to the grain boundaries. Since the dominant donors are

oxygen vacancies [22,23,40], V_{Zn} that act as acceptors diminish the effective doping concentration, so

$$N_{eff} = N_d - N_a. \tag{11}$$

The applied voltage during degradation is responsible for establishing an electric field that drags Zn atoms from the depletion region to the grain boundary. Consequently, new Zn vacancies appear in the grains that are detected with PALS technique. An increase in Zn vacancies implies an effective doping decrease after sample degradation. Thus, we conclude that many reported degradation processes (for commercial varistors) reflect into the formation of V_{Zn} in the grains and the Zn migration to the grain boundaries.

Gupta et al. proposed a similar model but not including Zn vacancy creation [4,18]. In particular, they explained their results with an ion-migration model in which the applied bias induces migration of Zn interstitials to the grain boundary reducing the concentration of zinc vacancies. The implications for the electrical behaviour, of these two models, are the same as in both a reduction of band bending and of effective doping concentration is proposed. However, our PALS experiments indicate that, after degradation, the density of V_{Zn} in the grains increases affecting the effective dopant concentration.

In previous works, we had determined from spectroscopy measurements that after degradation, especially using current pulses, the effective donor concentration increases [13]. We interpreted those results as the formation of oxygen vacancies after a very strong electric stress. So far, we have tested here the consequences of a relatively mild degradation to observe that the first stage in the degradation process involves the formation of Zn vacancies and the decrease of the barriers heights.

On the other hand, the effects of HCI degradation over the same type of varistors show significant differences with respect to the results obtained for the LCI degradation process. Indeed, after the HCI degradation, the capacitance increases by a factor of 2.1. Following a similar analysis, as before, the dopant concentration showed an increase of about 2.4 times. Thus, the donor density had to be incremented in the process. PALS results could be interpreted as the HCI degradation leads to the transformation of the V_{Zn}-like defects (present in the un-degraded varistors) to Zn–O divacancies. In a recent work, it was found that Zn–O divacancy formation energy increases with the Fermi level [35]. This behaviour is usually expected for a donor-type defect, so the Zn–O divacancy could be assumed to be a donor. Under this scenario, a stronger degradation entails the diminution of the acceptor-type defects and the increase of the donor-type concentration causing an effective doping increase with respect to the un-degraded varistor (see Equation (11)). However, this change in the defect-type nature is not sufficient to explain the strong increase in the dopant concentration observed in the HCI degraded samples. This should be related to the formation of a significant amount of donor-type defects, such as oxygen vacancies as previously stated. Moreover, a fraction of these defects could bind to the present V_{Zn}-like defects to form the Zn–O divacancies.

Conclusions

During a mild degradation process of zinc oxide-based varistors, new Zn vacancies appear in the grains as determined with PALS. The effective doping concentration tends

to decrease after sample degradation as a consequence of the Zn vacancies acceptor nature. The reduction of the barrier heights implies that Zn is drifted to the grain boundaries. Electrical measurements carried out with impedance spectroscopy technique were consistent with the results obtained using PALS and indicate that the doping concentration changes after degradation. However, for the HCI degradation, we found an increase in doping, indicating that eventually oxygen vacancies form outnumbering the effect of Zn vacancies of acceptor behaviour.

Funding

This work was partially supported by Agencia Nacional de Promoción Científica y Tecnológica (Argentina) (PICT 2011-1088), Consejo Nacional de Investigaciones Científicas y Técnicas (Argentina) (PIP # 114-200801-00444 and PIP # 112-201101-00793), Comisión de Investigaciones Científicas de la Provincia de Buenos Aires and SECAT-UNICEN.

References

[1] M. Seitz, F. Hampton and W. Richmond, *Additives and interfaces in electronic ceramics*, in *Advanced in Ceramics*, Vol. 7, M.F. Yan and A.H. Heuer, eds., The American Ceramic Society Inc., Columbus, 1983, p.60.
[2] D.R. Clarke J. Am. Ceram. Soc. 82 (1999) p.485.
[3] L.M. Levinson and H.R. Philipp, Am. Ceram. Soc. Bull. 65 (1986) p.639.
[4] T.K. Gupta, J. Am. Ceram. Soc. 73 (1990) p.1817.
[5] A. Bui, H.T. Nguyen and A. Loubiere, J. Phys. D: Appl. Phys. 28 (1995) p.774.
[6] M.A. Ramírez, M. Cilense, P.R. Bueno, E. Longo and J.A. Varela, J. Phys. D: Appl. Phys. 42 (2008) p.015503.
[7] R. Parra, M.A. Ponce, C.M. Aldao and M.S. Castro, J. Eur. Ceram. Soc. 27 (2007) p.3907.
[8] Z.Y. Lu, A.B. Glot, A.I. Ivon and Z.Y. Zhou, J. Eur. Ceram. Soc. 32 (2012) p.3801.
[9] M.A. Ramírez, W. Bassi, R. Parra, P.R. Bueno, E. Longo and J.A. Varela, J. Am. Ceram. Soc. 91 (2008) p.2402.
[10] M.A. Ramírez, W. Bassi, P.R. Bueno, E. Longo and J.A. Varela, J. Phys. D: Appl. Phys. 41 (2008) p.122002.
[11] M.A. Ramírez, A.Z. Simões, P.R. Bueno, M.A. Márquez, M.O. Orlandi and J.A. Varela, J. Mater. Sci. 41 (2006) p.6221.
[12] M.S. Castro and C.M. Aldao, Ceram. Int. 22 (1996) p.39.
[13] M.A. Ponce, M.A. Ramírez, R. Parra, C. Malagú, M.S. Castro, P.R. Bueno and J.A. Varela, J. Appl. Phys. 108 (2010) p.074505.
[14] P. Hautojärvi and C. Corbel, *Positron spectroscopy of defects*, in *Metals and Semiconductors, in Positron Spectroscopy of Solids. International School of Physics "Enrico Fermi", Course CXXV*, A. Dupasquier and A.P. Mills Jr., eds., IOS Press, Amsterdam, 1995, p.491.
[15] A. Dupasquier, R. Ferragut, M.M. Iglesias, M. Massazza, G. Riontino, P. Mengucci, G. Barucca, C.E. Macchi and A. Somoza, Philos. Mag. 87 (2007) p.3297.
[16] A. Dupasquier, G. Kögel and A. Somoza, Acta Mater. 52 (2004) p.4707.
[17] R. Krause-Rehberg and H.S. Leipner, *Positron Annihilation in Semiconductors, Defect Studies, Springer Series in Solid-State Sciences 127*, Springer, Berlin, 1999.
[18] T.K. Gupta, W.D. Straub, M.S. Ramanachalam, J.P. Schaffer and A. Rohatgi, J. Appl. Phys. 66 (1989) p.6132.
[19] M.S. Ramanachalam, A. Rohatgi, J.P. Schaffer and T.K. Gupta, J. Appl. Phys. 69 (1991) p.8380.

[20] A. Janotti and C.G. Van de Walle, Rep. Prog. Phys. 72 (2009) p.126501.
[21] M.D. McCluskey and S.J. Jokela, J. Appl. Phys. 106 (2009) p.071101.
[22] F. Tuomisto, V. Ranki, K. Saarinen and D.C. Look, Phys. Rev. Lett. 91 (2003) p.205502.
[23] A. Zubiaga, F. Plazaola, J.A. García, F. Tuomisto, V. Muñoz-Sanjosé and R. Tena-Zaera, Phys. Rev. B 76 (2007) p.085202.
[24] Z.Q. Chen, M. Maekawa, A. Kawasuso, S. Sakai and H. Naramoto, Physica B 376 (2006) p.722.
[25] G. Brauer, J. Kuriplach, J. Cizek, W. Anwand, O. Melikhova, I. Prochazka and W. Skorupa, Vacuum 81 (2007) p.1314.
[26] Z.Q. Chen, S. Yamamoto, M. Maekawa, A. Kawasuso, X.L. Yuan and T. Sekiguchi, J. Appl. Phys. 94 (2003) p.4807.
[27] F. Tuomisto, K. Saarinen, K. Grasza and A. Mycielski, Phys. Stat. Sol. (B) 243 (2006) p.794.
[28] F. Tuomisto, A. Mycielski and K. Grasza, Superlattices Microstruct. 42 (2007) p.218.
[29] J. Zhong, A.H. Kitai, P. Mascher and W. Puff, J. Electrochem. Soc. 140 (1993) p.3644.
[30] G. Brauer, W. Anwand, W. Skorupa, J. Kuriplach, O. Melikhova, C. Moisson, H. von Wenckstern, H. Schmidt, M. Lorenz and M. Grundmann, Phys. Rev. B. 74 (2006) p.045208.
[31] G. Brauer, W. Anwand, W. Skorupa, J. Kuriplach, O. Melikhova, J. Cizek, I. Prochazka, C. Moisson, H. von Wenckstern H. Schmidt, M. Lorenz and M. Grundmann, Superlattices Microstruct. 42 (2007) p.259.
[32] S. Brunner, W. Puff, A.G. Balogh and P. Mascher, Mat. Sci. Forum 363–365 (2001) p.141.
[33] G.E. Pike, Phys. Rev. B 30 (1984) p.795.
[34] G.D. Mahan, J. Appl. Phys. 54 (1983) p.3825.
[35] R. Vidya, P. Ravindran, H. Fjellvåg, B.G. Svensson, E. Monakhov, M. Ganchenkova and R.M. Nieminen, Phys. Rev. B 83 (2011) p.045206.
[36] S.M. Sze, *Physics of Semiconductor Devices*, Wiley, New York, 1981.
[37] K. Kao, *Dielectric Phenomena in Solids*, Elsevier Academic Press, San Diego, 2004.
[38] C.R. Crowell and V.L. Rideout, Solid State Electron. 12 (1969) p.89.
[39] P. Kirkegaard, N.J. Pedersen and M. Eldrup, *PATFIT-88 program, Tech. Rep. M-2740*, Riso National Laboratory, Roskilde, 1989.
[40] P. Hautojärvi, *Positrons in Solids, Topics in Current Physics*, Vol. 12, Springer, Heidelberg, 1979.
[41] A. Dupasquier, R. Romero and A. Somoza, Phys. Rev. B 48 (1993) p.9235.
[42] B. Oberdorfer and R. Würschum, Phys. Rev. B 79 (2009) p.184103.
[43] P. Hautojärvi, Mater. Sci. Forum 47 (1995) p.175–178.
[44] J. Kuriplach, G. Brauer, O. Melikhova, J. Cizek, I. Prochazka and W. Anwand, Mater. Res. Soc. Symp. Proc. 1201 (2010) p.H02–03.
[45] E.H. Rhoederick and R.H. Williams, *Metal–Semiconductor Contacts*, Clarendon Press, Oxford, 1988.
[46] M.A. Ponce, M.S. Castro and C.M. Aldao, J. Mater. Sci. Mater. Elecctron. 20 (2009) p.25.
[47] F. Schipani, C.M. Aldao and M.A. Ponce, AIP Adv. 2 (2012) p.032138.